Sol–Gel Preparation and Third-Order Nonlinear Optical Properties of TiO_2 Thin Films

Tadanori HASHIMOTO, Toshinobu YOKO,* and Sumio SAKKA
Institute for Chemical Research, Kyoto University, Uji, Kyoto 611
(Received October 25, 1993)

Rutile and anatase thin films have been prepared by the sol–gel method using $Ti(OC_3H_7{}^i)_4$. Third-order nonlinear optical properties of both TiO_2 thin films have been investigated by the third-harmonic generation (THG) method and the effect of the polymorph of TiO_2 on the third-order nonlinear optical susceptibility, $\chi^{(3)}$, has been examined. The measured $\chi^{(3)}$ values of rutile and anatase thin films were 1.4×10^{-12} and 9.7×10^{-13} esu, respectively. The $\chi^{(3)}$ values corrected for the porosity of the film were 4.0×10^{-12} (rutile) and 2.4×10^{-12} esu (anatase), which are about 100 times as high as that of SiO_2 glass used as standard sample (2.8×10^{-14} esu). The measured and corrected $\chi^{(3)}$ values were discussed in comparision with those calculated on the basis of several models.

As previously reported,[1] the third-order nonlinear optical susceptibility, $\chi^{(3)}$, of the sol–gel derived α-Fe_2O_3 thin film was 5.8×10^{-11} esu, which is about 2000 times as high as that of SiO_2 glass (2.8×10^{-14} esu). This was ascribed to the much higher refractive index of α-Fe_2O_3 than that of SiO_2 glass on the basis of Miller's rule[2,3] which predicts that a material with high refractive index shows a high $\chi^{(3)}$.

TiO_2 is also considered to be a promising nonlinear optical material because of the high refractive index more than 2.5[4] and high transparency in the visible region. In fact, $\chi^{(3)}$ values of 1.5×10^{-12} and 3.1×10^{-12} esu for a TiO_2 single crystal, which were measured by nearly degenerate three-wave mixing (TWM)[5] and degenerate four-wave mixing (DFWM)[6,7] methods, respectively, have been reported. There are, however, no comparative studies on the third-order nonlinear optical properties of TiO_2 polymorphs except a theoretical study by Lines[8] dealing with the contribution of empty d orbital as well as sp orbitals to linear and nonlinear optical properties.

In the present study, TiO_2 thin films of rutile and anatase phases have been prepared on the SiO_2 glass substrates by the sol–gel method. Third-order nonlinear optical properties of both TiO_2 films have been investigated by THG method and the effect of the polymorph of TiO_2 on the third-order nonlinear optical susceptibility has been examined.

Experimental

Preparation of TiO_2 Thin Films. TiO_2 thin films were prepared by the sol–gel method. As starting solutions, $Ti(OC_3H_7{}^i)_4$–i-C_3H_7OH–H_2O–$HN(CH_2CH_2OH)_2$ and $Ti(OC_3H_7{}^i)_4$–i-C_3H_7OH–H_2O–HNO_3 solutions were selected for rutile and anatase films, respectively. The chemical compositions of the solutions were 1 : 20 : 1 : 1 and 1 : 20 : 1 : 0.1 in molar ratio, respectively. The difference between these two solutions is whether the solution includes diethanolamine ($HN(CH_2CH_2OH)_2$, DEA) or HNO_3. In the former solution, titanium tetraisopropoxide ($Ti(OC_3H_7{}^i)_4$, TTIP) was first dissolved in a solution of DEA and half of a prescribed amount of isopropyl alcohol (i-C_3H_7OH). Then, the solution was mixed with a solution of H_2O and the remainder of i-C_3H_7OH. For the latter solution, TTIP was first diluted by half of a prescribed amount of i-C_3H_7OH. Then, the solution was mixed with a solution of HNO_3aq containing a given amount of H_2O and the remainder of i-C_3H_7OH. Both coating solutions were allowed to stand at 30 °C for 2 h prior to use.

Dip-coating was used for film formation. A SiO_2 glass substrate was immersed in a coating solution, and pulled up at a rate of 3 cm min^{-1}. The film was heated at 400, 500, 650, or 800 °C for 10 min immediately after each coating procedure. This cycle was repeated 10 times to attain the desired film thickness of about 0.3 μm. To enhance the laser-induced damage threshold (LIDT),[9] a SiO_2 coating was further applied onto the TiO_2 film. Otherwise, a part of TiO_2 film peeled off upon laser irradiation. In the present coating process, films are formed on both surfaces of the SiO_2 glass substrate. The TiO_2 and additional SiO_2 films on one surface were removed to minimize the interference effect[10] of THG light in the THG measurement.

Characterization of TiO_2 Thin Films. The crystalline phases precipitated in the TiO_2 thin films were identified by X-ray diffraction method using Cu Kα radiation. The refractive indices of TiO_2 films were determined by an ellipsometer in the wavelength region from 500 to 1000 nm. The ellipsometry measurement also gave the film thickness. The absorption spectra of TiO_2 films with and without additional SiO_2 coating were measured in the wavelength region from 200 to 2000 nm by a UV-visible spectrophotometer.

THG measurements of TiO_2 thin films were made by means of a nonlinear optical measurement apparatus (Tokyo Instruments, Inc., Tokyo, Japan). The Q-switched Nd : YAG laser was operated at the fundamental wavelength of 1064 nm with a pump pulse duration of 10 ns and a peak power density of 200 MW cm^{-2}. The laser frequency at 1900 nm was obtained directly by stimulated Raman scattering in a high pressure hydrogen cell, which was excited by the Nd : YAG line at 1064 nm. The THG light at 633 nm, which was isolated by a monochromator, was detected by a photomultiplier connected to a box-car integrator. The sample was mounted on a goniometer and rotated at 0.25° intervals from −40 to +40° by a computer-controlled stepper motor with respect to the axis perpendicular to the incident light.

In both absorption spectrum and THG measurements, the samples were irradiated from the side without films.

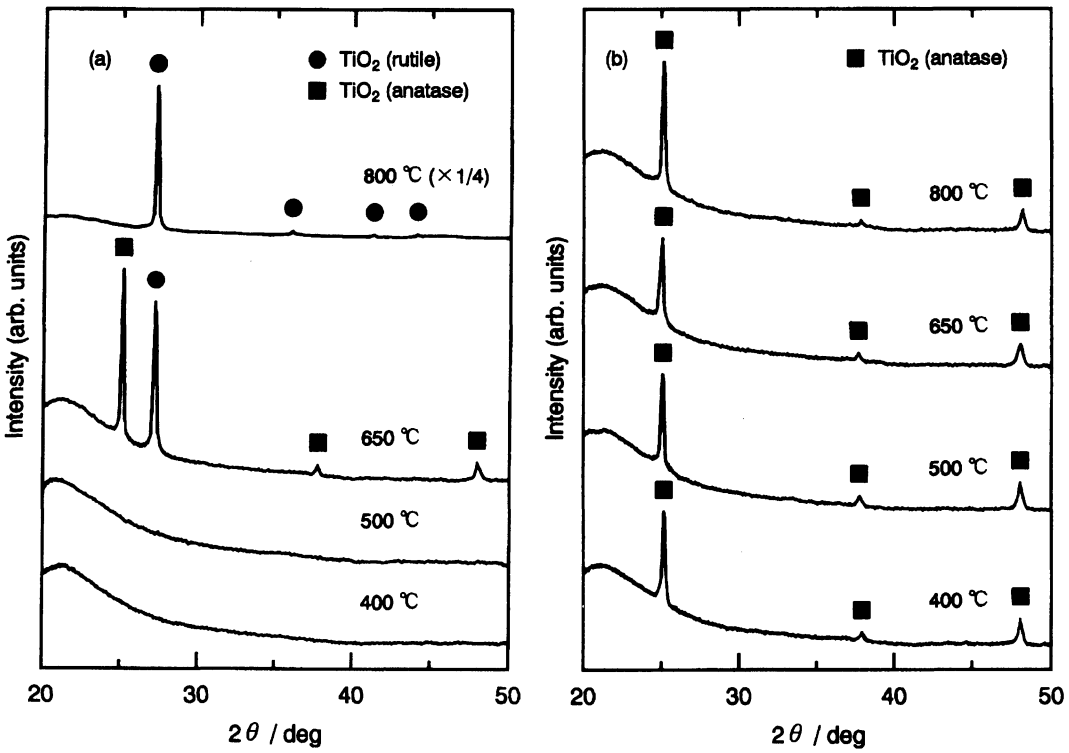

Fig. 1. X-Ray diffraction patterns of TiO_2 thin films prepared from solutions containing (a) DEA and (b) HNO_3.

Results

Crystallization Behavior. Figure 1 shows X-ray diffraction patterns of TiO_2 thin films prepared from solutions containing (a) DEA and (b) HNO_3. The films prepared from a solution containing DEA were amorphous below 500 °C, and consisted of a mixture of anatase and rutile phases at 650 °C and a single phase of rutile at 800 °C. On the other hand, the films prepared from a solution containing HNO_3 were crystallized into a single phase of antase at 400 °C and no changes in the crystalline phase and the X-ray diffraction peak intensity were seen above 500 °C. The crystallite size in the TiO_2 films prepared from the solutions containing DEA and HNO_3 was 45—55 nm and 35—45 nm, respectively.

Rutile and anatase films which were prepared by heating at 800 °C were selected for measurements of various optical properties.

Refractive Index and Optical Transmittance. The wavelength dependence of refractive index, n, for TiO_2 thin films is shown in Fig. 2. It is seen that the refractive indices of both TiO_2 films decrease with increasing wavelength and the refractive index of rutile film is higher than that of anatase film as well known. Figure 3 presents linear plots of $(n^2-1)^{-1}$ versus E^2 for TiO_2 thin films based on Wemple's equation[11]

$$\frac{1}{n^2-1} = \frac{E_0}{E_d} - \frac{E^2}{E_0 E_d}, \tag{1}$$

where E, E_0, and E_d are the photon energy, the average oscillator energy and dispersion energy in eV unit, respectively. E_0 and E_d are important optical properties of materials.[11] The refractive indices were estimated as $n_{3\omega}=2.40$ at 633 nm and $n_\omega=2.27$ at 1900 nm, and the coherence length, $l_c=1.9/[6(n_{3\omega}-n_\omega)]$, was 2.3 μm for the rutile film. In a similar manner, $n_{3\omega}$, n_ω, and l_c for the anatase film were estimated as 2.29, 2.16, and 2.4 μm, respectively. The thickness of the TiO_2 films obtained by 10 dippings was typically 0.30—0.35 μm.

From refractive indices, n_s and n_p, of single crystals[4,12] and porous thin films, the porosities, p, of both TiO_2 films can be estimated as follows:[13]

$$p = \left(1 - \frac{n_p^2 - 1}{n_s^2 - 1}\right) \times 100(\%), \tag{2a}$$

and

$$n_s = \sqrt[3]{n_o^2 n_e}, \tag{2b}$$

where n_s corresponds to a radius of refractive index sphere having the same volume as that of a refractive index ellipsoid with the two n_o radii and one n_e radius (o: ordinary ray, e: extraordinary ray) for uniaxial crystals such as rutile and anatase. The porosities of rutile and anatase films were estimated as 22.6 and 19.9 %, respectively.

Figure 4 shows the absorption spectra of TiO_2 thin films with and without additional SiO_2 coating. All spectra have a number of mountains and troughs arising from the interference of light. The larger amplitude of interference spectra of rutile film compared with anatase film results from the higher refractive index of

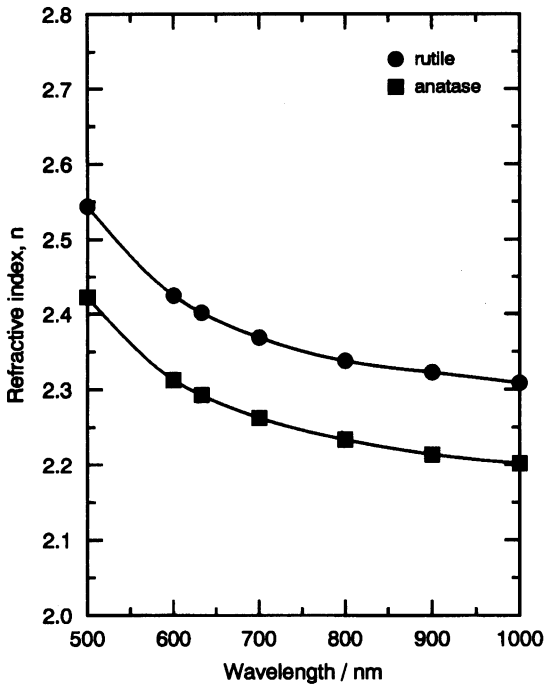

Fig. 2. Wavelength dependence of refractive index, n, for TiO_2 thin films.

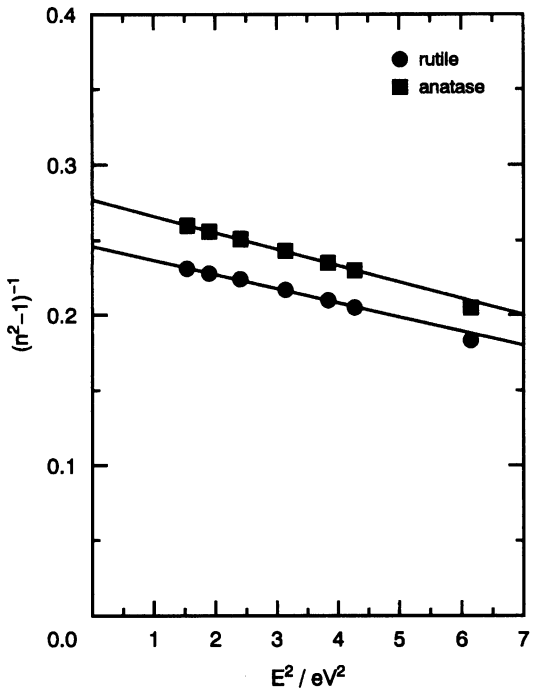

Fig. 3. Linear plots of $(n^2-1)^{-1}$ versus E^2 for TiO_2 thin films.

the former. It is seen that the additonal SiO_2 coating reduces the optical loss due to reflection especially in the wavelength region above about 400 nm. The optical band gaps, E_g, of rutile and anatase films were estimated to be 3.0 and 3.2 eV, respectively, corresponding to an energy between the conduction band, which predominantly has a Ti 3d character, and the O 2p valence band.[14] These values are in good accordance with those reported previously.[15]

Evaluation of $\chi^{(3)}$ Values. The THG intensities as a function of the rotation angle are given for (a) rutile film, (b) anatase film and (c) SiO_2 glass in Fig. 5. The THG intensity patterns of both TiO_2 films clearly shows the interference between the THG lights from TiO_2 film and SiO_2 glass substrate as previously reported.[10] The THG intensity was obtained by the least squares method as solid line in Fig. 5.

In the present study, $\chi^{(3)}$ values were determined by the equation[16]

$$\chi^{(3)}_{\text{film}} = \frac{2}{\pi}\chi^{(3)}_{\text{SiO}_2}\frac{l_{\text{c,SiO}_2}}{l}\sqrt{\frac{I_{3\omega,\text{film}}}{I_{3\omega,\text{SiO}_2}}} \times\sqrt{\frac{n^3_{\omega,\text{film}}n_{3\omega,\text{film}}T^3_{\omega,\text{SiO}_2}T_{3\omega,\text{SiO}_2}}{n^3_{\omega,\text{SiO}_2}n_{3\omega,\text{SiO}_2}T^3_{\omega,\text{film}}T_{3\omega,\text{film}}}}\ (\text{esu}), \tag{3}$$

where I denotes the THG peak intensity. The film thickness is used for l, because the film thickness is less than the coherence length. The values of $\chi^{(3)}_{\text{SiO}_2}=2.8\times10^{-14}$ esu and $l_{\text{c,SiO}_2}=18.1$ μm were used for SiO_2 glass as both standard sample and substrate.[17]

The intensity of THG signal generated from TiO_2 film was determined by the equation[10]

$$I_{\text{film}} = \frac{I_{\max}+I_{\min}}{2} - \frac{I_{\text{substrate}}}{2} = \frac{I_{\max}+I_{\min}}{2} - \frac{I_{\text{SiO}_2}}{2}, \tag{4}$$

where $I_{\max}$ and $I_{\min}$ are the upper and lower envelopes of the superimposed THG intensity pattern. The contribution of THG light from the additional SiO_2 film on the TiO_2 film was neglected, because the $\chi^{(3)}_{\text{SiO}_2}$ is low and the thickness of SiO_2 film (less than about 0.2 μm) is much smaller than the coherence length. The $\chi^{(3)}$ values of rutile and anatase films were determined to be 1.4×10^{-12} and 9.7×10^{-13} esu, respectively. Table 1 summarizes the optical properties of TiO_2 thin films.

The accuracy of the present THG measurement for thin film samples is estimated to be $\chi^{(3)}$ $l\approx3\times10^{-13}$ esu μm from the weakest THG intensity that can be resolved into two components of film and substrate. This value agrees with the value of 3×10^{-13} esu μm reported by Kubodera et al.[10]

Discussion

Rutile[4] and anatase[12] have values of about 0.3 and −0.1, respectively, for the birefrigence, $\Delta n=n_e-n_o$. This means that TiO_2 has a large optical anisotropy. However, in the present sol–gel derived TiO_2 thin films crystallites are very small in size and randomly oriented, as seen in Fig. 1, and so the film can be regarded as almost optically isotropic material. Therefore, the present analysis and interpretation concerning the refractive index and $\chi^{(3)}$ are made based on the isotropic values.

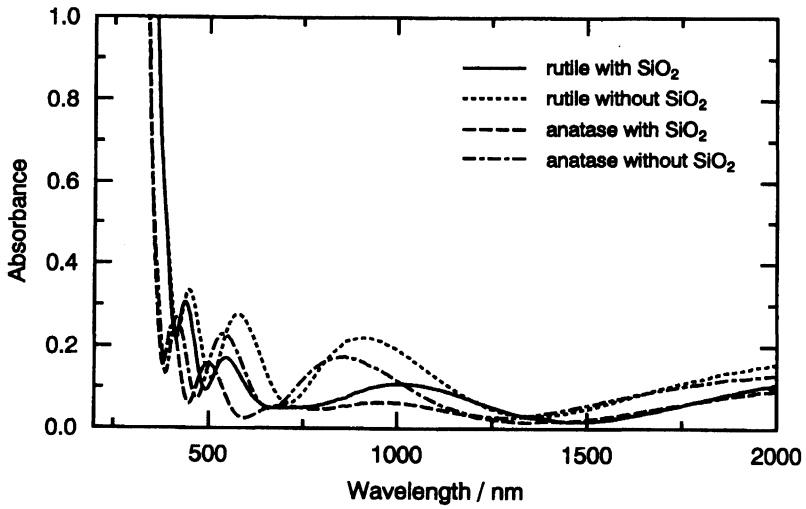

Fig. 4. Absorption spectra of TiO_2 thin films with and without additional SiO_2 coating.

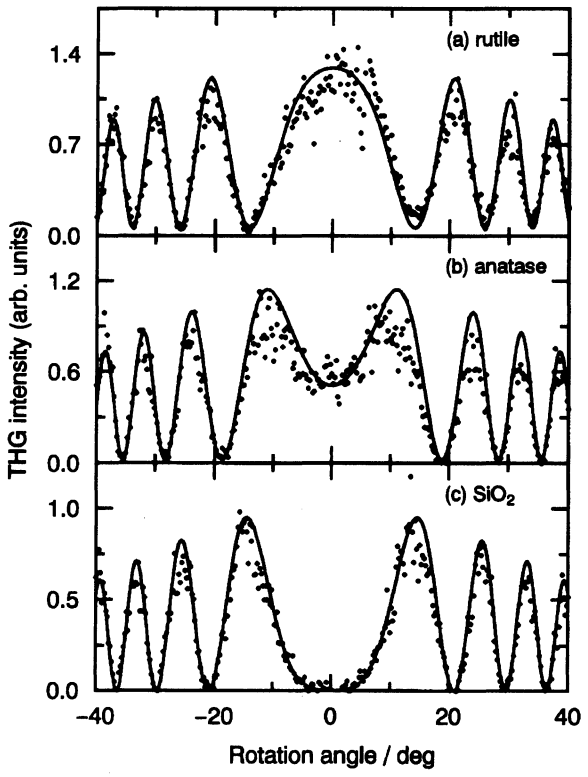

Fig. 5. THG intensities as a function of rotation angle for (a) rutile film, (b) anatase film, and (c) SiO_2 glass. Solid line is the best fitted curve for the plotted data.

Relationship between $\chi^{(3)}$ and Refractive Index, n. It is possible to estimate $\chi^{(3)}$ of a material from refractive index, n, according to Miller's rule[2,3]

$$\chi^{(3)} = \left[\chi^{(1)}\right]^4 \times 10^{-10}(\text{esu}), \tag{5a}$$

and

$$\chi^{(1)} = \frac{n^2 - 1}{4\pi}. \tag{5b}$$

The $\chi^{(3)}$ values of 1.2×10^{-12} and 7.3×10^{-13} esu, which are predicted by Miller's rule for rutile and anatase thin films, respectively, as in the third row of Table 2, are in good accordance with the measured $\chi^{(3)}$ values, 1.4×10^{-12} and 9.7×10^{-13} esu, as in the first row.

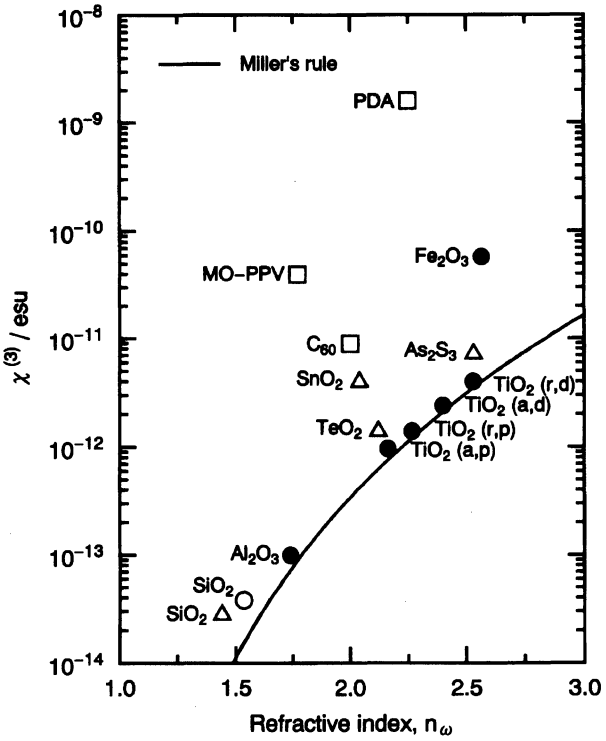

Fig. 6. Relationship between $\chi^{(3)}$ and refractive index, n_ω, at 1900 nm for TiO_2 thin films and other nonlinear optical materials.[1,16–23] Circle, triangle and square denote inorganic crystal, inorganic amorphous material, and organic material, respectively. Closed circles are the data measured by the present authors. The letters of r, a, d, and p in parentheses denote rutile, anatase, dense, and porous, respectively. PDA: polydiacetylene, MO-PPV: poly(2,5-dimethoxy *p*-phenylene vinylene).

Since the present sol–gel derived TiO_2 thin films are

Table 1. Optical Properties of TiO_2 Thin Films

	$n_{3\omega}$	n_ω	$T_{3\omega}$ %	T_ω %	E_0 eV	E_d eV	E_g eV	p %	$I_{3\omega,\mathrm{film}}/I_{3\omega,\mathrm{SiO_2}}$	l_c μm	l μm	$\chi^{(3)}$ esu
Rutile	2.40	2.27	86.5	81.0	5.1	20.7	3.0	22.6	0.22	2.3	0.35	1.4×10^{-12}
	(2.68)	(2.53)			(5.2)	(27.6)						
Anatase	2.29	2.16	91.3	82.6	5.0	18.1	3.2	19.9	0.10	2.4	0.30	9.7×10^{-13}
	(2.51)	(2.40)			(5.7)	(26.6)						

The data in parentheses are the values of single crystals[4,12] calculated by Wemple's equation[11] under the isotropic assumption. Transmittance is the value of TiO_2 thin films with additional SiO_2 coating.

Table 2. Comparison of $\chi^{(3)}$ Values of TiO_2 Thin Films Measured and Calculated by Several Empirical Equations

	$\chi^{(3)}$/esu	
	Rutile	Anatase
Measured values (porous)	1.4×10^{-12}	9.7×10^{-13}
Corrected values (dense)	4.0×10^{-12}	2.4×10^{-12}
Miller's rule (porous)[2,3]	1.2×10^{-12}	7.3×10^{-13}
Miller's rule (dense)	3.4×10^{-12}	2.1×10^{-12}
Calculated values by Eq. 8 (dense)	3.4×10^{-12}	2.3×10^{-12}
Lines' model (porous)[8]	2.3×10^{-12}	1.7×10^{-12}
Lines' model (dense)	4.7×10^{-12}	2.7×10^{-12}

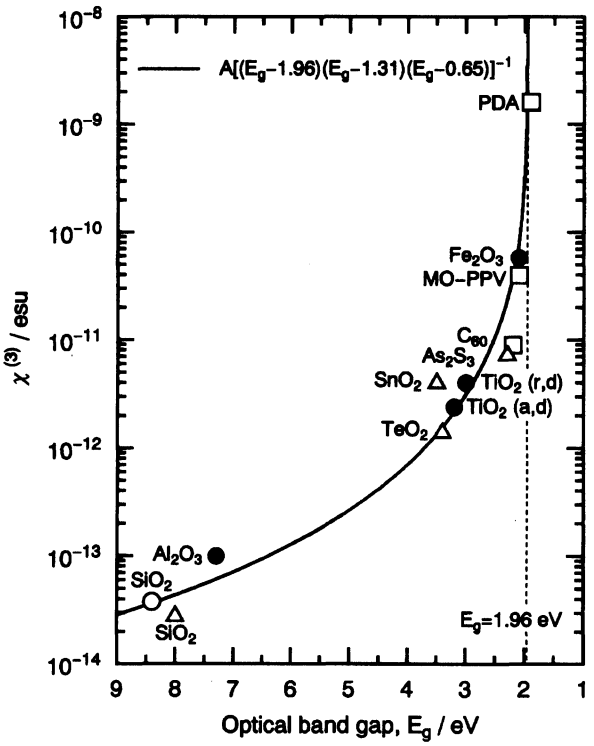

Fig. 7. Relationship between $\chi^{(3)}$ and optical band gap, E_g, for TiO_2 thin films and other nonlinear optical materials. References and notations are the same as in Fig. 6.

porous in nature, it is of essence to estimate the $\chi^{(3)}_{\mathrm{dense}}$ values of hypothetical dense films corrected for porosity, p. This can be accomplished by combining Eqs. 2 and 5 as follows:

$$\chi^{(3)}_{\mathrm{dense}} = \chi^{(3)}_{\mathrm{porous}} \left(\frac{100}{100-p}\right)^4 (\mathrm{esu}). \quad (6)$$

The $\chi^{(3)}_{\mathrm{dense}}$ values of 4.0×10^{-12} and 2.4×10^{-12} esu for rutile and anatase dense films, respectively, as in the second row of Table 2 are about 100 times as high as $\chi^{(3)}$ of SiO_2 glass as standard sample, 2.8×10^{-14} esu. The $\chi^{(3)}_{\mathrm{dense}}$ value of rutile is in reasonable accordance with $\chi^{(3)}(-\omega;\omega,\omega,-\omega)$ of 1.5×10^{-12} esu (TWM)[5] and 3.1×10^{-12} esu (DFWM)[6,7] reported previously if one assumes that the $\chi^{(3)}(-\omega;\omega,\omega,-\omega)$ corresponds to $\chi^{(3)}(-3\omega;\omega,\omega,\omega)$ obtained by the THG method.

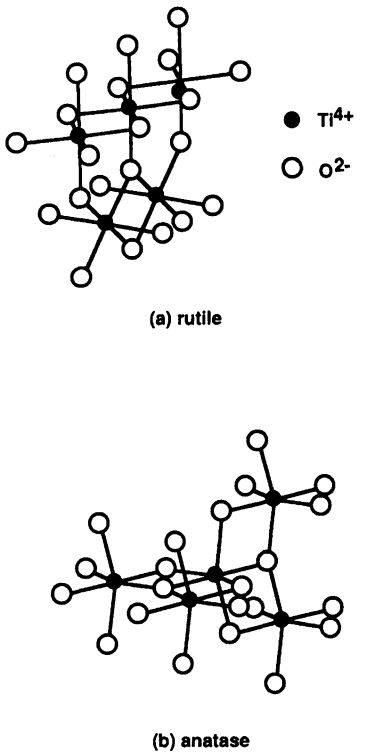

Fig. 8. Structures of (a) rutile and (b) anatase.

Figure 6 shows a relationship between $\chi^{(3)}$ and refractive index, n_ω, at 1900 nm for TiO_2 thin films and other nonlinear optical materials reported so far.[1,16—23] It is seen that inorganic materials with high refractive index inherently exhibit high optical nonlinearlity.

The $\chi^{(3)}$ values of organic polymers such as polydi-

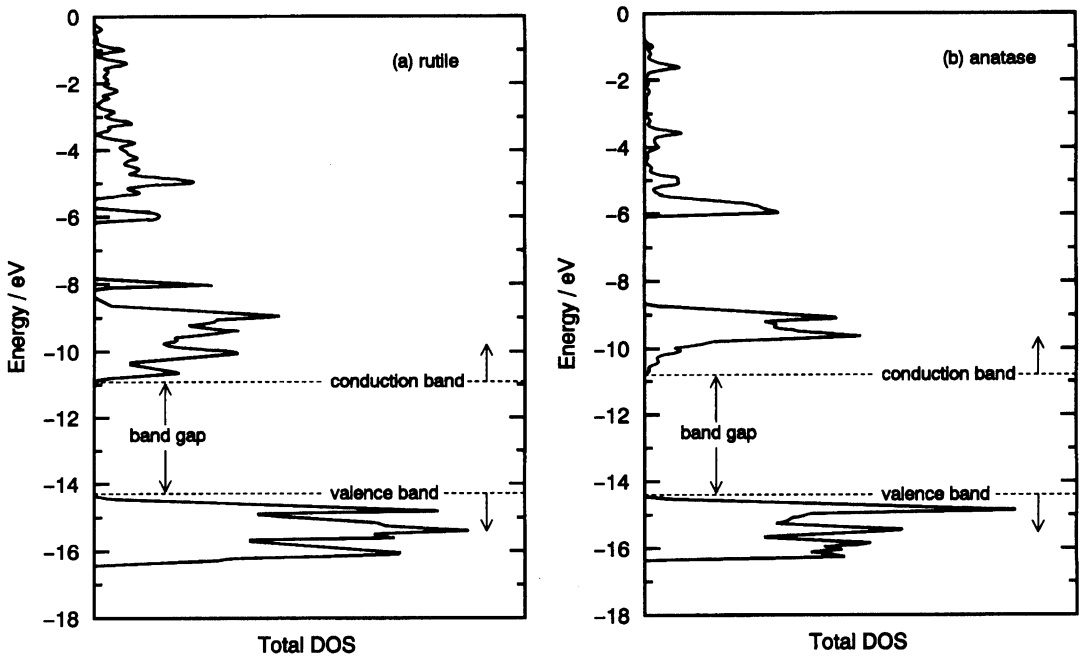

Fig. 9. Density of states (DOS) for (a) rutile and (b) anatase after Ref. 26.

acetylene (PDA)[21] and poly(2,5-dimethoxy *p*-phenylene vinylene) (MO-PPV)[22] deviate from the relation to a considerable extent, due to the enhancement by the so-called three-photon resonance or near three-photon resonance.[24] Since the measured $\chi^{(3)}$ includes the significant contribution of the imaginary part, there are no simple relations between $\chi^{(3)}$ and refractive index for these organic materials, that is, Miller's rule does not hold.

Relationship between $\chi^{(3)}$ and Optical Band Gap, E_g. One can expect that an enhancement in $\chi^{(3)}(-3\omega;\omega,\omega,\omega)$ occurs when in a material a frequency of interacting light approaches either one of one-, two- or three-photon resonance frequencies according to the relation[24]

$$\chi^{(3)}(-3\omega;\omega,\omega,\omega) \propto \frac{N}{\hbar^3}\sum_{gnmn'}\rho(g)F(\omega)\Omega_{gn}\Omega_{nm}\Omega_{mn'}\Omega_{n'g}(\text{esu}), \quad (7a)$$

and

$$F(\omega) = \frac{1}{(E_{ng}-3\omega)(E_{mg}-2\omega)(E_{n'g}-\omega)} + \frac{1}{(E_{ng}+\omega)(E_{mg}-2\omega)(E_{n'g}-\omega)} + \frac{1}{(E_{ng}+\omega)(E_{mg}+2\omega)(E_{n'g}-\omega)} + \frac{1}{(E_{ng}+\omega)(E_{mg}+2\omega)(E_{n'g}+3\omega)}, \quad (7b)$$

where $\rho(g)$, E_{ij} and Ω_{ij} are the density matrix element of fundamental state, the energy difference between states i and j in $\hbar$ ($=h/2\pi$, h: Planck's constant) unit and the transition matrix elements between states i and j, respectively. For materials having optical band gap, E_g, higher than three-photon energy, 3ω, the three-photon resonance makes the greatest contribution to the enhancement of $\chi^{(3)}$. Then, to a good approximation, the most significant term due to the three-photon resonance in Eq. 7 may be expressed as follows:

$$\chi^{(3)} = \frac{A}{(E_g-1.96)(E_g-1.31)(E_g-0.65)}\ (\text{esu}), \quad (8)$$

where A is the phenomenological constant.

Figure 7 gives a relationship between $\chi^{(3)}$ and optical band gap, E_g, for TiO_2 thin films and other nonlinear optical materials shown in Fig. 6. In Fig. 7, for organic materials the absorption edge of exciton absorption is used instead of E_g. Taking into account that E_g should not depend on the porosity, the corrected $\chi^{(3)}$ values for TiO_2 thin films are plotted as a function of E_g. In this figure, the $\chi^{(3)}$ values of these materials show a clear tendency to increase asymptotically as the E_g approaches 1.96 eV corresponding to the photon energy of THG signal. This change obeys Eq. 8 when the parameter, A, takes a value of 1.4×10^{-11}. From this equation, $\chi^{(3)}$ values were estimated to be 3.4×10^{-12} and 2.3×10^{-12} esu for rutile and anatase, respectively, as in the fifth row of Table 2, which are also in good accordance with the corrected $\chi^{(3)}$ values, 4.0×10^{-12} and 2.4×10^{-12} esu, as in the second row.

Calculation of $\chi^{(3)}$ Based on Lines's Model. Lines introduced a bond-orbital theory dealing with the contribution of empty d orbital in addition to sp orbitals to linear and nonlinear optical properties, giving the following equation to estimate $\chi^{(3)}$:[8,25]

$$\chi^{(3)} = \frac{25 \times 10^{-13} d^2 \left(n_\omega^2 - 1\right) f_L^3 E_S^6}{3\pi \left[E_S^2 - E^2\right]^4} \text{ (esu)}, \quad (9)$$

where d denotes the bond length between cation and anion, $f_L = (n_\omega^2 + 2)/3$ the Lorentz local-field correction factor, E_S the Sellmeier gap which is in practice equal to the average oscillator energy, E_0, in Eq. 1. From Eq. 9, one can obtain $\chi^{(3)}$ values of 4.7×10^{-12} and 2.7×10^{-12} esu for rutile and anatase dense films, respectively, as in the seventh row of Table 2, which are in good accordance with the corrected values, 4.0×10^{-12} and 2.4×10^{-12} esu, as in the second row.

Therefore, the much higher $\chi^{(3)}$ values of both TiO_2 polymorphs compared with SiO_2 glass can be ascribed to the higher refractive index and the narrower optical band gap or Sellmeier gap of the former, which all result from the significant contribution of Ti 3d orbital due to the large p–d overlapping in the short Ti–O bond length of 1.95—1.96 Å.[26]

Comparison of $\chi^{(3)}$ between Rutile and Anatase. The difference in crystal structure between both TiO_2 polymorphs is that the two edges shared TiO_6 octahedra form straight chains in rutile, as distinct from the zigzag chains consisting of four edges shared TiO_6 octahedra in anatase as seen from Fig. 8. A band structure calculation reveals that the straight chains of TiO_6 octahedra in rutile give rise to two important results of the broader t_{2g} part of Ti 3d conduction band which lies around −9.5 eV of the density of states (DOS), and the higher DOS around the bottom of the conduction band compared with anatase (Fig. 9).[26] On the other hand, the noticeable difference in O 2p valence band around −15.5 eV between both TiO_2 polymorphs is not seen. The broader conduction and explains the narrower optical band gap, and the higher refractive index due to the higher optical transition probability of rutile than that of anatase. The higher DOS around the bottom of conduction band also gives rise to the higher optical transition probability of rutile compared with anatase. In fact, it has been reported that the optical transition between O 2p valence band and Ti 3d conduction band is direct for rutile, whereas it is indirect for anatase.[27] Since the THG process requires the same parity as linear optical transition, the higher $F(\omega)$ and Ω_{ij} in Eq. 7 resulting from the characteristic DOS of rutile is considered to be responsible for the slightly higher $\chi^{(3)}$ value of rutile compared with anatase.

Summary

The third-order nonlinear optical properties of the sol–gel derived TiO_2 thin films of rutile and anatase phases have been investigated by the THG method, and the effect of the polymorph of TiO_2 on the third-order nonlinear optical susceptibility has been examined. The following results were obtained.

(1) The measured $\chi^{(3)}$ values of rutile and anatase thin films were 1.4×10^{-12} and 9.7×10^{-13} esu, respectively. The $\chi^{(3)}$ values corrected for porosity were 4.0×10^{-12} (rutile) and 2.4×10^{-12} esu (anatase), which are about 100 times as high as that of SiO_2 glass.

(2) The much higher $\chi^{(3)}$ values of both TiO_2 polymorphs compared with SiO_2 glass were ascribed to the higher refractive index and the narrower optical band gap of the former due to the significant contribution of Ti 3d orbital as a result of the large p–d overlapping in the short Ti–O bond length of 1.95—1.96 Å.

(3) The slightly higher $\chi^{(3)}$ value of rutile compared with anatase was also attributed to the higher refractive index and the narrower optical band gap of the former, which both possibly arise from the broader Ti 3d conduction band as a result of the formation of the straight chains of TiO_6 octahedra in rutile, as distinct from the zigzag chains of TiO_6 octahedra in anatase.

References

1) T. Hashimoto, T. Yoko, and S. Sakka, *J. Ceram. Soc. Jpn.*, **101**, 64 (1993).
2) R. C. Miller, *Appl. Phys. Lett.*, **5**, 17 (1964).
3) C. C. Wang, *Phys. Rev. B*, **2**, 2045 (1970).
4) J. R. DeVore, *J. Opt. Soc. Am.*, **41**, 416 (1951).
5) R. Adair, L. L. Chase, and S. A. Payne, *Phys. Rev. B*, **39**, 3337 (1989).
6) E. M. Vogel, S. G. Kosinski, D. M. Krol, J. L. Jackel, S. R. Friberg, M. K. Oliver, and J. D. Powers, *J. Non-Cryst. Solids*, **107**, 244 (1989).
7) E. M. Vogel, M. J. Weber, and D. M. Krol, *Phys. Chem. Glass*, **32**, 231 (1991).
8) M. E. Lines, *Phys. Rev. B*, **43**, 11978 (1991).
9) K. H. Guenther, T. W. Humpherys, J. Balmer, J. R. Bettis, E. Casparis, J. Ebert, M. Eichner, A. H. Guenther, E. Kiesel, R. Kuehnel, D. Milam, W. Ryseck, S. C. Seitel, A. F. Stewart, H. Weber, H. P. Weber, G. R. Wirtenson, and R. M. Wood, *Appl. Opt.*, **23**, 3743 (1984).
10) K. Kubodera and H. Kobayashi, *Mol. Cryst. Liq. Cryst.*, **182A**, 103 (1990).
11) S. H. Wemple, *J. Chem. Phys.*, **67**, 2151 (1977).
12) H. E. Merwin, "International Critical Tables of Numerical Data, Physics, Chemistry, and Technology, VII," ed byE. W. Washburn, C. J. West, N. E. Dorsey, and M. D. Ring, (1931), p.16.
13) B. E. Yoldas, *Appl. Opt.*, **19**, 1425 (1980).
14) K. Vos, *J. Phys. C*, **10**, 3917 (1977).
15) M. Grätzel and F. P. Rotzinger, *Chem. Phys. Lett.*, **118**, 474 (1985).
16) H. Nasu, K. Kubodera, M. Kobayashi, M. Nakamura, and K. Kamiya, *J. Am. Ceram. Soc.*, **73**, 1794 (1990).
17) G. R. Meredith, B. Buchalter, and C. Hanzlik, *J. Chem. Phys.*, **78**, 1533 (1983).
18) G. R. Meredith, *Phys. Rev. B*, **24**, 5522 (1981).
19) N. Ueda, H. Kawazoe, Y. Watanabe, M. Takata, M. Yamane, and K. Kubodera, *Appl. Phys. Lett.*, **59**, 502 (1991).
20) S. H. Kim, T. Yoko, and S. Sakka, *J. Am. Ceram. Soc.*, **76**, 2486 (1993).

21) T. Kanetake, K. Ishikawa, T. Hasegawa, T. Koda, K. Takeda, M. Hasegawa, K. Kubodera, and H. Kobayashi, *Appl. Phys. Lett.*, **54**, 2287 (1989).
22) T. Kurihara, Y. Mori, T. Kaino, H. Murata, N. Takada, T. Tsutsui, and S. Saito, *Chem. Phys. Lett.*, **183**, 534 (1991).
23) J. S. Meth, H. Vanherzeele, and Y. Wang, *Chem. Phys. Lett.*, **197**, 26 (1992).
24) F. Kajzar and J. Messier, "Nonlinear Optical Properties of Organic Molecules and Crystals, 2," ed by D. S. Chemla and J. Zyss, Academic Press, New York (1987), p. 51.
25) M. E. Lines, *Phys. Rev. B*, **41**, 3383 (1990).
26) J. K. Burdett, T. Hughbanks, G. J. Miller, J. W. Richardson, Jr., and J. V. Smith, *J. Am. Chem. Soc.*, **109**, 3639 (1987).
27) T. Yoko, A. Yuasa, K. Kamiya, and S. Sakka, *J. Electrochem. Soc.*, **138**, 2279 (1991).